

~~The influence of mesoscale climate drivers on hypoxia in a fjord-like deep coastal inlet and its potential implications regarding climate change and greenhouse gas production: examining a decade of water quality data~~

5

The influence of mesoscale climate drivers on hypoxia in a fjord-like deep coastal inlet and its potential implications regarding climate change: examining a decade of water quality data

Johnathan Daniel Maxey^{1,2}, Neil D. Hartstein², Aazani Mujahid³, Moritz Müller¹

10 ¹Faculty of Engineering, Computing and Science, Swinburne University of Technology, Kuching 93350, Malaysia

²ADS Environmental Services, Kota Kinabalu, Sabah, 88400, Malaysia

³Faculty of Resource Science & Technology, University Malaysia Sarawak, Kota Samarahan 94300, Sarawak, Malaysia

Correspondence to: Johnathan Daniel Maxey (jdaniel@adseser.com)

Abstract.

15 Deep coastal inlets are sites of high sedimentation and organic carbon deposition that account for 11% of the world's organic carbon burial. Australasia's mid to high latitude regions have many such systems. It is important to understand the role of climate forcings in influencing hypoxia and organic matter cycling in these systems, but many such systems, especially in Australasia, remain poorly described.

20 We analysed a decade of *in-situ* water quality data from Macquarie Harbour, Tasmania, a deep coastal inlet with more than 180,000 tons of organic carbon loading per annum. Monthly dissolved oxygen, total Kjeldahl nitrogen, dissolved organic carbon, and dissolved inorganic nitrogen concentrations were significantly affected by rainfall patterns. Increased rainfall was correlated to higher organic carbon and nitrogen loading, lower oxygen concentrations in deep basins, and greater oxygen concentrations in surface waters. Most notably, the Southern Annular Mode (SAM) significantly influenced oxygen distribution in the system. High river flow (associated with low SAM index values) impedes deep water renewal as the primary mechanism driving basin water hypoxia. Climate forecasting ~~predicted~~ predicts increased winter rainfall and decreased summer rainfall, which may further exacerbate hypoxia in this system.

30 Currently, ~~Macquarie~~the Harbour's basins experience frequent (up to 36% of the time) and prolonged (up to 2 years) oxygen-poor conditions ~~that with the potential to may~~ promote greenhouse gas (CH₄, N₂O) production ~~a~~ Increased

~~greenhouse gas production will alter~~ing the processing of organic matter entering the system. The increased winter rainfall predicted for the area ~~will potentially increase greenhouse gas emissions due to~~will likely promote increased spread and duration of hypoxia in the basins. Further understanding of these systems and how they respond to climate change will improve our estimates of future organic matter cycling (burial vs export) ~~and greenhouse gas production~~.

35 **1 Introduction**

Fjords and fjord-like estuaries (also called Deep Coastal Inlets – DCI; Keith *et al. et al.*, 2020) are sites of high sedimentation and organic carbon (OC) burial. These systems account for approximately 11% of the world's annual OC burial (Smith *et al. et al.*, 2015). Compared to other marine benthic environments (*e.g.* sediments along the continental shelf, deeper pelagic sediments, shallow-water carbonate sediments), they bury the most OC per unit area (Smith *et al. et al.*, 2015; Bianchi *et al. et al.*, 2018, 2020).

Their location within mid to high latitude coastal margins and disproportionate role in geochemical cycling make these systems especially vulnerable to anthropogenic pressure (Walinsky *et al. et al.*, 2009; Gilbert *et al. et al.*, 2010; Bianchi *et al. et al.*, 2018, 2020). Bianchi *et al. et al.*, (2018) have classified fjord and fjord-like DCIs as "Aquatic Critical Zones" in need of further investigation, especially regarding how they might respond to changes in climatological drivers and anthropogenic pressure. One of the critical issues facing coastal environments is the expansion of poor oxygen conditions due to increased anthropogenic organic matter loadings (Diaz and Rosenberg, 2008; Oschlies *et al. et al.*, 2018; Breitbart *et al. et al.*, 2018; Pitcher *et al. et al.*, 2021).

Combined effects of environmental drivers or forcings drive the distribution of dissolved oxygen (DO) in any given system. In fjord and fjord-like DCIs, this includes wind, tidal exchange, river flow, organic loading, deep water renewal (DWR) (Edwards and Edelsten, 1977; Gade and Edwards, 1980; Geyer and Cannon, 1982) and microbial processing in the sediments and water column (Gillibrand *et al. et al.*, 2006; Maxey *et al. et al.*, 2020). Characteristics of these systems are shallow sills at their mouth and several sills or ridges that separate the estuary into various basins (Pickard and Stanton, 1980; Stanton and Pickard, 1980; Inall and Gillibrand, 2010). These morphological features restrict mixing and promote stratification of the water column by isolating basin waters from exchange mechanisms between the coastal ocean and surrounding catchment (Inall and Gillibrand, 2010). Hypoxia (*defined as* DO concentrations below 2 mg L⁻¹) has been long recognised and can be a natural feature of these systems (Rosenberg, 1977; Rabalais *et al. et al.*, 2010, Inall and Gillibrand, 2010; Ji *et al. et al.*, 2020).

60

The availability of DO influences the eventual fate of OC processed by microbial communities as it enters either aerobic or anaerobic metabolic pathways (*see* del Giorgio and Williams, 2005). In addition, the cycling of organic matter and nutrients

in poor oxygen environments often leads to the production of potent greenhouse gasses such as methane (CH₄) and nitrous oxide (N₂O) (Codispoti *et al.*, 2005). The fate of carbon exported to marine systems from estuaries is tied to oxygen distribution. Estuarine morphology, physical oceanography, and anthropogenic impacts (*e.g.* hydroelectric dams, land-use modification, sewage outfalls, etc.) drive the oxygen distribution.

Understanding how DO distribution and availability in fjord-like systems respond to climate change requires understanding how ~~it~~ they currently responds to changes in local and mesoscale environmental drivers. These drivers include rainfall and runoff and associated nutrient and organic matter loading. Predicted climate change impacts include changes in air pressure, wind strength, rainfall patterns, and storm intensity (Grose *et al.*, 2010; Priestley and Catto, 2021; Goyal *et al.*, 2021), all of which have the potential to affect DO distribution in fjord-like estuaries (Austin and Inall, 2002; Gillibrand *et al.*, 2005, 2006; Austin and Inall 2011; Hartstein *et al.*, 2019).

Understanding how broader environmental drivers affect localised DO distribution requires spatially extensive long-term datasets which are not readily available in many systems. Ideally, these datasets would provide enough statistical power to tease out relationships between external drivers (*e.g.* rainfall volume, rainfall accumulation, OC and organic nitrogen (ON) loading, river flow and climate oscillation indices) and DO distribution through the water column. A 10-year dataset is available for a relatively remote DCI on Tasmania's West Coast, enabling analyses focusing on long-term trends in water quality, freshwater and organic matter loading, and their relationships with climate drivers.

The aims of this paper are to:

1. Understand the effects of rainfall or freshwater inputs on OM loading, nutrient loading, and DO distribution in a fjord-like deep coastal inlet.
2. Describe the current effects that broader climate oscillations have on DO distribution and discuss implications future climate predictions have on possible DO dynamics in these systems (example of a restricted sill system), especially regarding physical drivers of deep water renewal.
3. Discuss implications for managing these systems regarding the regulation of freshwater input, OM loading, and the potential to promote oxygen poor conditions favouring GHG emissions.

Formatted: Not Highlight

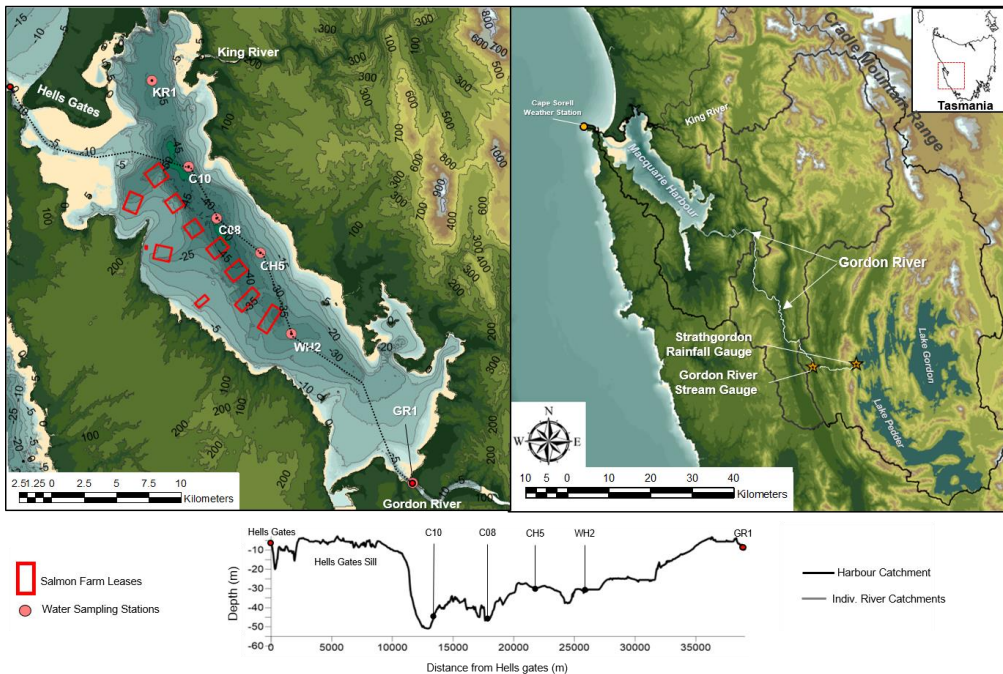
2 Methods

95 2.1 Study Area

Macquarie Harbour is a fjord-like DCI located on the West Coast of Tasmania. Although it's glacially carved status of the Harbour itself is somewhat unclear (Baker and Ahmad, 1959; Kiernan, 1990, 1991, 1995), it has the morphology and resulting oceanographic dynamics shared by many fjords and fjord-like systems, including a propensity for oxygen-poor basins (Creswell *et al.*, 1989; Hartstein *et al.*, 2019). Descriptions of its DO drivers (Hartstein *et al.*, 2019 and Maxey *et al.*, 2017, 2020) suggest disparate processes affecting surface water and basin DO distribution. Namely, DO in the basin waters is resupplied by DWR. Where or when the direct effects of these processes wane, diffusive mixing and water column oxygen demand become the key drivers of oxygen availability (Inall and Gillibrand, 2010; Hartstein *et al.*, 2019; Maxey *et al.*, 2020).

105 The Harbour is oriented in an NW by SE direction, is approximately 33 km long, 9 km wide, and has a surface area of 276 km². Compared to the rest of Australia, Western Tasmania receives some of the highest rainfall (more than 2,500 mm year⁻¹) and high seasonal rainfall variability (Dey *et al.*, 2018). As a result, broad-scale climate oscillations like the Southern Annual Mode (SAM) (Meneghini, Simmonds, and Smith, 2007; Hill, Santoso, & England, 2009) affect westerly winds that generate orographic rainfall in Macquarie Harbour's catchment. Since the 1970s, both the SAM index (positive values associated with stronger westerlies) and winter rainfall in Macquarie Harbour's catchment have increased (Taschetto & England, 2009; Marshall *et al.*, 2018; Fogt and Marshall, 2020).

115 The primary source of fresh water to the Harbour is the Gordon River which is responsible for up to 82% of the system's freshwater input (Hartstein *et al.*, 2019). The mouth of the Gordon River is located on the Harbour's SE end and drains a combined catchment (including the Franklin River) of 5,682 km² (MHDOWG, 2014). This catchment is located west of the Cradle Mountain Range (**Figure 1**). At the NW end of the Harbour, the King River is the second largest contributor of fresh water to the system and drains a catchment area of 802 km².



120 **Figure 1: Macquarie Harbour, Tasmania.** Monthly sampling sites shown with red circles, Gordon River Stream Gauge and Strathgordon Rainfall Gauge shown as orange stars. Aquaculture lease boundaries are shown as hollow red rectangles. Lease locations are sourced from Land Information Systems Tasmania (LISTmap - <https://maps.thelist.tas.gov.au/>). Station names reflect general harbour locations where KR1 indicates King River 1; C10, C08, CH5 indicate Central Harbour 10, 08, 5; WH2 indicates World Heritage Area 2; and GR1 indicates Gordon River station 1.

125 River flow in the upper catchments of the Gordon and King rivers has been regulated by hydroelectric dams since 1983
 (operated by Hydro Tasmania). Gordon River mean flow has been reported to range from 190 to 265 m³ sec⁻¹ and the King
 River at approximately 55 m³ sec⁻¹ (Carpenter *et al et al.*, 1991; Koehnken, 2006). More recent analyses indicate that mean
 monthly flows can vary significantly, with flows < 100 m³ sec⁻¹ observed in summer and early autumn and 500 m³ sec⁻¹ in
 late autumn, winter, and spring (Hartstein *et al et al.*, 2016; Maxey *et al et al.*, 2020). Daily peak flow can reach over 1500
 130 m³ sec⁻¹. However, before the introduction of hydroelectric dams, peak flow could have been greater (King, 1980; King and
 Tyler, 1981; King and Tyler, 1982; Walker, 1985).

Both rivers supply dark, tannin-rich waters, limiting the system's photic zone to the first 2-3 m of the water column (Carpenter *et al.*, 1991; Edgar *et al.*, 1999). These tannin-rich waters are a product of high organic matter loading, estimated at up to 180,000 tons OC per year (Hartstein *et al.*, 2016; Maxey *et al.*, 2020).

While the Harbour's catchments are largely undeveloped native forest, anthropogenic inputs include treated copper mining discharges from the King River and several commercial salmon farms situated within the Harbour's centre. Salmon farming has been present in the Harbour since the 1980s. Between 2009 and 2016, it underwent significant expansion from 9000 tonnes to 16,000 tonnes. Since 2016 farm biomass has been set at 9,500 tonnes (Dept Natural Resources and Environment Tasmania <https://salmonfarming.nre.tas.gov.au>) (see **Figure 1** for an overview of farming leases). It has been suggested by MHDOWG (2014) and Hartstein *et al.*, (2016) that Gordon River dam releases may introduce highly concentrated OM pulses into the system when reservoir levels are low. Increased OM loading can impact pelagic oxygen demand in the harbour as shown by Maxey *et al.*, (2020).

Macquarie Harbour has a strongly stratified water column set up by a long (14 km), shallow (< 3m in areas) constricted sill and oxygen-poor basins (Cresswell *et al.*, 1989; Maxey *et al.*, 2017). Temperature differences above and below the halocline can be 10 °C. However, temperatures in the bottom waters exhibit little variability (2 to 3 degrees) (Hartstein *et al.*, 2019). Basin waters are refreshed episodically by DWR, which is driven by a combination of low atmospheric pressure, low harbour water level, and sustained NW winds (Hartstein *et al.*, 2019). However, the relative importance of freshwater supply to DWR and oxygen distribution remains unknown.

Climate change models reviewed and presented in Grose *et al.*, (2010) and Bennett *et al.*, (2010) indicate that the west coast of Tasmania, including the main rainwater catchments feeding Macquarie Harbour, is expected to experience increased storm intensity, wetter winters, and drier summers (up to 10% to 18% wetter or drier throughout the catchment). However, there has been a steady increase in spring and winter rainfall in Western Tasmania (Taschetto & England, 2009) despite increasing SAM index values (Marshall *et al.*, 2018). There is still a need to clarify the specific impacts of a changing climate on rainfall patterns. Nevertheless, to predict how future climate scenarios might affect harbour dynamics, it is vital to understand how the system currently responds to present drivers.

Much of the previous literature describing the oceanography and environmental status of Macquarie Harbour has focused on the effects of copper mine discharge (Carpenter *et al.*, 1991; Koehnken, 1996; Featherstone *et al.*, 1997; Stauber *et al.*, 2000; Eriksen *et al.*, 2001; Teasdale *et al.*, 2003, Augustinus *et al.*, 2010; Cracknell *et al.*, 2019). Recently, Hartstein *et al.*, 2019 and Maxey *et al.*, 2020) have expanded the understanding of the physical and biological oceanography (initially described by Cresswell *et al.*, 1989) of the Harbour. They found that DWR is the major driver of bottom water oxygen distribution and that Gordon River organic loading is the primary driver of pelagic

oxygen demand (POD). These previous studies demonstrate that external physical drivers (i.e. rainfall patterns, sea level, air pressure, wind direction and speed, etc) establish horizontal and vertical salinity, density, light and nutrient availability gradients in this system. Da Silva *et al. et al.*, (2021) examined the microbial communities present in ~~the~~ Macquarie Harbour's water column. They showed distinct functional groups along the harbour's salinity and depth gradients, suggesting that ~~external-elimati~~physical drivers may also influence harbour microbial processes.

Formatted: Font: Italic

2.2 Data Collection and Analysis

Water quality data are available from a monthly water quality monitoring program (since October 2011). The monitoring data examined here included sonde profiles and *in-situ* water samples taken at several sites within the Harbour (**Figure 1** and **Table 1**). These include stations at end members and within each of the Harbour's basins. After its initial stages (2011 to 2013) the sampling program was expanded to include additional sites and parameters (**Table 1**).

Water quality sonde profiles were collected every meter using a YSI-6600 V2 equipped with optical DO (accuracy from 0 to 20 mg L⁻¹ is ± 0.1 mg L⁻¹ or 1% of reading whichever is greater; precision is 0.01 mg L⁻¹), salinity (accuracy ± 0.1 PPT or 1% of reading whichever is greater; precision is 0.01 PPT), temperature (accuracy is ± 0.15 °C; precision is 0.01 °C), and depth sensors. Sonde calibration was checked and corrected (when needed) each sampling period. Water samples were collected at various depths (see **Table 1**) using a 5 L Niskin bottle sampler. Water sample parameters include total organic carbon (TOC) and dissolved organic carbon (DOC), total Kjeldahl nitrogen (TKN), soluble ammonia (NH₃), nitrate (NO₃), and chlorophyll-a. Water collected for soluble inorganic N was filtered immediately using 0.45 µm polyethersulfone syringe filters (Whatman Puradisc), and all samples were stored in a chilled dark container until being transported to the lab for analysis.

Analytical Services Tasmania analysed all water samples. Maxey *et al. et al.*, (2020) outlined detailed organic carbon and chlorophyll-a methodologies. Dissolved NH₃, NO₃, and TKN were analysed using a Lachat Flow Injection Analyser. NH₃ and NO₃ analyses used methods based on APHA Standard methods (2005) 4500-NH₃ H (reporting limit 0.005 mg L⁻¹) and 4500 - NO₃ I (reporting limit 0.002 mg L⁻¹). TKN was determined by converting N into (NH₄)₂SO₄ using K₂SO₄ digestion and reacting this digested sample with alkaline buffer, salicylate and hypochlorite to form a coloured compound to be read on the Lachat analyser (reporting limit 0.1 mg L⁻¹).

Table 1: Monthly sampling stations showing coordinates, starting months of individual parameters, and sampling depth (in meters).

Station	Depth (m) (MSL)	Dissolved Oxygen / Salinity	NPOC	TKN	NH ₃	NO ₃	CHL- a
KR1 361316, 5325972	35	Oct 2011 Every Meter	-	July 2014 2, 10, 20, B2	Oct 2011 2, 10, 20, B2	Oct 2011 2, 10, 20, B2	Dec 2011 2, 12
C10 363708, 5320464	44	Dec 2013 Every Meter	July 2014 Every Meter	Dec 2013 2, 10, 20, B2	Dec 2013 2, 10, 20, B2	Dec 2013 2, 10, 20, B2	Sep 2014 2
C08 365489, 5317238	47	Dec 2013 Every Meter	-	Sep 2014 20, B2	Dec 2013 20, B2	Dec 2013 20, B2	Dec 2013 2, 12
CH5 368215, 5315124	39	Oct 2013 Every Meter	-	Oct 2013 1, 2, 10, 20, B2	Oct 2013 1, 2, 10, 20, B2	Oct 2013 1, 2, 10, 20, B2	Oct 2013 2, 12
WH2 370218, 5309894	32	Oct 2011 Every Meter	July 2014 1, 2, 5, 10, 15, 20, 30, B2	Oct 2011 1, 2, 5, 10, 15, 20, 30, B2	Oct 2011 1, 2, 5, 10, 15, 20, 30, B2	Oct 2011 1, 2, 5, 10, 15, 20, 30, B2	Dec 2011 2, 12
GR1 377784, 5300603	12	July 2014 Every Meter	July 2014 2, B2	Dec 2013 2, B2	Dec 2013 2, B2	Dec 2013 2, B2	Dec 2013 2

*Station coordinates given in UTM (Zone 55G)
Dates indicate starting month of sampling parameter
Sampling depths indicated under each date with B2 = 2m from seabed*

205 The Bureau of Meteorology (BOM) provided rainfall and stream gauge data from several gauging locations within the Gordon River catchment, namely Strathgordon rainfall gauge station and the Gordon Above Denison stream gauge (hereafter referred to as “Gordon River Stream Gauge”; **Figure 1**). Daily rainfall and streamflow data were available for the entire span of the monthly water quality program, and the Strathgordon rainfall dataset extends back until the 1970s. Rainfall data were organised into several metrics, including daily average monthly rainfall and total accumulated rainfall 30, 20, 10, 5, 3, 2 days and one day before each monthly monitoring sampling period. The seasonality of rainfall was analysed using a two-way ANOVA grouping data by year and season. *Post hoc* analyses were performed using TUKEY HSD.

210

The flow was estimated at the mouth of the Gordon River (for loading estimations) by scaling daily rainfall to the size of the catchment and assuming a rainfall and runoff coefficient of 0.70 adopted from a neighbouring catchment with similar land cover, geology, and slope (Willis, 2008). Additional streamflow from Gordon River dam releases was estimated by subtracting scaled rainfall contributions to river flow measured at the Gordon River Stream Gauge. This flow was added to the estimated runoff entering the Harbour. OC and N loading from the Gordon River was determined by multiplying the parameter concentration by the estimated flow entering the Harbour.

215

220

The relationship between rainfall (of various metrics), riverine OC and N loading, and water quality (*e.g.* DO concentration and salinity) was analysed using Pearson correlations for each site, for each 1 m depth bin, and the entirety of the water quality dataset. In heavily stratified systems, the surface layer's depth depends upon freshwater supply, tidal forcing, and atmospheric pressure (*i.e.* thicker freshwater lens during flood events) (Gillibrand *et al. et al.*, 2005; Cage *et al. et al.*, 2006; Inall and Gillibrand, 2011). When comparing sonde profiles over multiple sampling periods, surface referenced data have a shifting datum due to the varying thickness of the freshwater lens and thus introduce a source of error in the analysis. To reduce this possible source of error, we arranged the water quality data to reference height from the seabed (not depth from the surface) when comparing it to catchment rainfall and river flow.

225

230

Hypoxic volume was estimated by scaling up monthly DO concentrations using a 1 m vertical resolution box model. Oxygen concentrations within each box were represented by data from individual monitoring stations located in the boxes. A representative volume was assigned to each station's box by using the harbour hypsography in 1 m bins (bathymetry data were provided by Lucieer *et al. et al.*, 2007 and Hartstein *et al. et al.*, 2016). To estimate the hypoxic volume in the system, we assumed DO concentrations within the box did not vary. DO concentrations below 10 m depth were then multiplied by each bin's representative volume of water.

235

3 Results

3.1 Rainfall Patterns (2011-2021)

The average daily river flow measured from the Gordon River Stream Gauge (Dennison Flow) (see Figure 1) ranged from 17 m³ sec⁻¹ to 263 m³ sec⁻¹ (Figure 2A). Two-way ANOVAs revealed a significant seasonal and yearly effect (with significant interaction). Minimum daily average flows ranged from 17 m³ sec⁻¹ in 2012 to 117 m³ sec⁻¹ in 2013. Hydroelectric releases, and not catchment rainfall, would predominantly determine flow at the Gordon River Stream Gauge as the upstream catchment area between the dam and the gauge is relatively small (only 49.5 km², or about 0.8% of the size of the ungauged catchment area feeding the Gordon River).

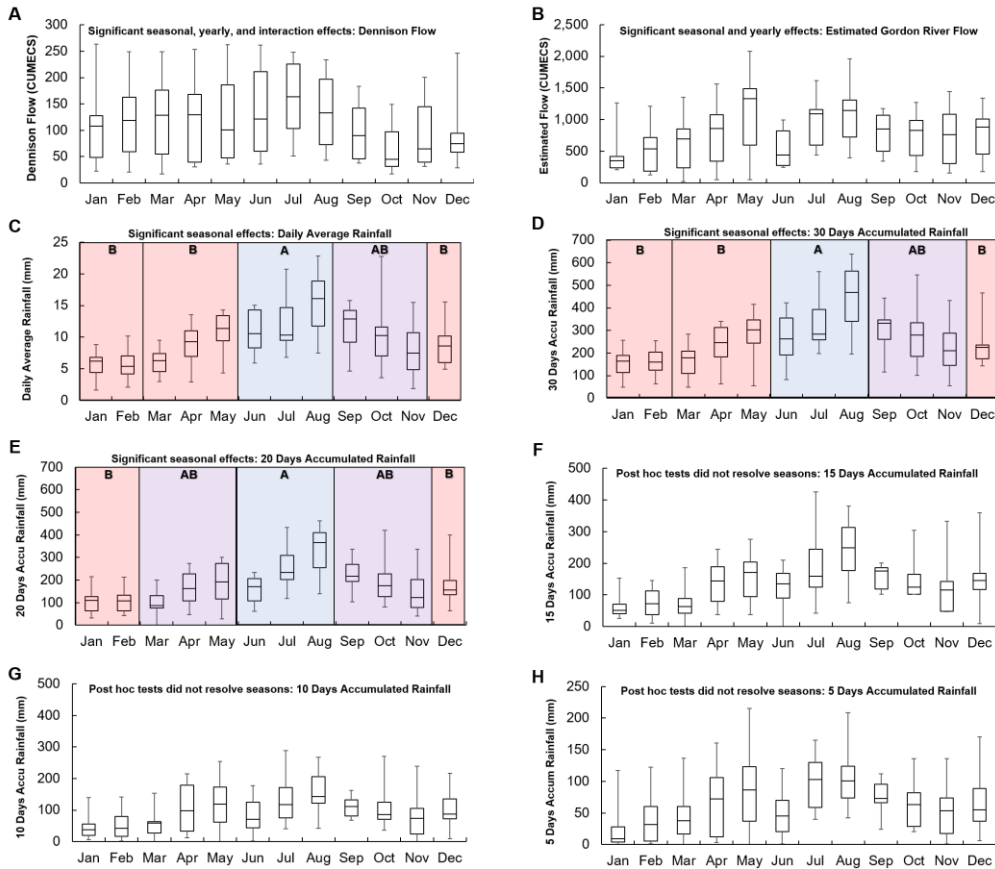
240

245 Estimated river flow into the harbour also exhibited statistically significant ($p = 0.04$) seasonal periods and significant ($p = 0.01$) interannual variation (Figure 2B). The average winter period daily flow was estimated to be $759 (\pm 67) \text{ m}^3 \text{ sec}^{-1}$. During summer, the estimated flow was approx. $502 (\pm 62) \text{ m}^3 \text{ sec}^{-1}$. The greatest estimated flow observed occurred in August 2018 at approx. $1,630 \text{ m}^3 \text{ sec}^{-1}$.

250 Significant seasonal patterns in rainfall were observed at the Strathgordon station with greater rainfall (daily average and accumulated) in winter (June – August; blue shading and Group A) (daily average $12.9 \pm 0.9 \text{ mm day}^{-1}$; Figure 2C) relative to summer (December – February; red shading and Group B) ($6.6 \pm 0.6 \text{ mm day}^{-1}$) and autumn (March - May) ($8.3 \pm 0.7 \text{ mm day}^{-1}$) (see Figure 2 and Table 1). *Post hoc* testing could not resolve a significant difference between spring (September – November; purple shading and Group AB) ($10.6 \pm 0.9 \text{ mm day}^{-1}$) and the other seasons (Figure 2C). Total accumulated rainfall before sampling also showed significant seasonal patterns when considering 30 days accumulated rainfall (Figure 2D) and 20 days accumulated rainfall (Figure 2E), but no seasonal pattern could be resolved when considering accumulation over 15 days (Figure 2F), 10 days (Figure 2G), or 5 days (Figure 2H). There were no significant interannual effects on rainfall at the Strathgordon station of any metric.

Formatted: Font: Not Bold

Formatted: Font: Not Bold



260 **Figure 2:** Box plots of flow and rainfall metrics from 2011 to 2021 including (A) Gordon River Stream Gauge flow, (B) Estimated daily flow into the Harbour, (C) Daily average rainfall at Strathgordon station, (D) 30 day, (E) 20 day, (F) 15 day, (G) 10 day, and (H) 5-day rainfall accumulation before monthly water quality sampling. *Post hoc* (Tukey HSD) groupings is-are depicted as colours and letters shown above within the plot area for datasets where two-way ANOVA revealed a significant seasonal effect (for instance Group A / Blue Shading indicates a significantly distinct group).

265

The average daily river flow measured from the Gordon River Stream Gauge (see Figure 1) ranged from $17 \text{ m}^3 \text{ sec}^{-1}$ to $263 \text{ m}^3 \text{ sec}^{-1}$ (Figure 2). Two-way ANOVAs revealed a significant seasonal and yearly effect (with significant interaction). Minimum daily average flows ranged from $17 \text{ m}^3 \text{ sec}^{-1}$ in 2012 to $117 \text{ m}^3 \text{ sec}^{-1}$ in 2013. Hydroelectric releases, and not

270 catchment rainfall, would predominantly determine flow at the Gordon River Stream Gauge as the upstream catchment area
271 between the dam and the gauge is relatively small (only 49.5 km², or about 0.8% of the size of the ungauged catchment area
272 feeding the Gordon River).

273 Estimated river flow into the harbour also exhibited statistically significant ($p = 0.04$) seasonal periods and significant ($p =$
274 0.01) interannual variation. The average winter period daily flow was estimated to be $759 (\pm 67) \text{ m}^3 \cdot \text{sec}^{-1}$. During summer,
275 the estimated flow was approx. $502 (\pm 62) \text{ m}^3 \cdot \text{sec}^{-1}$. The greatest estimated flow observed occurred in August 2018 at approx.
276 $1,630 \text{ m}^3 \cdot \text{sec}^{-1}$.

3.2 Rainfall Patterns and Water Quality at the Gordon River Mouth

280 At the mouth of the Gordon River, DOC and DON concentrations ranged from 4 mg L^{-1} to 21 mg L^{-1} in surface waters and 2
281 mg L^{-1} to 19.8 mg L^{-1} 2 m from the riverbed. Correlations between daily average rainfall and OC concentrations were
282 statistically significant but the effect size was stronger with samples taken 2 m off the seabed ($r = 0.70$, $p = 1.31 \times 10^{-13}$)
283 compared to surface water correlations ($r = 0.53$, $p = 1.53 \times 10^{-7}$; **Figure 3**). The relationship between OC and rainfall
284 accumulation was strongest five days before sampling ($r = 0.7$ OC). It should be noted that the correlation coefficient
285 between rainfall and bottom water OC concentration was relatively stable (and above 0.6) from 5 to 30 days of accumulation
286 before sampling.

DON concentrations at station GR1 ranged from 0.042 mg L^{-1} to 0.43 mg L^{-1} in surface waters and from 0.134 mg L^{-1} to
287 0.46 mg L^{-1} 2 m from the riverbed. As observed with the OC samples, ON concentrations were significantly correlated with
288 rainfall, although the strength of this relationship was more modest in comparison. Daily average rainfall correlation
289 coefficients from surface and bottom samples ranged from $r = 0.33$ ($p = 0.0062$) to 0.47 ($p = 8.0 \times 10^{-5}$) respectively. The
290 strongest correlation observed between rainfall and DON concentration was found using rainfall accumulation five days
291 prior to sampling ($r = 0.65$).

Rainfall and estimated flow were significantly correlated with TKN (greatest observation was $r = 0.65$, 5 days accumulation)
292 and NO_3^- concentrations (greatest was $r = -0.64$ 10 days prior to sampling). The nature of the relationships between rainfall
293 and NO_3^- concentration differed based on water sampling depth. Correlations between rainfall and NO_3^- concentrations 2 m
294 off the riverbed were positive (strongest relationship $r = 0.49$, 5 days accumulation before sampling), but surface water
295 concentrations were negatively correlated (strongest relationship $r = -0.64$, 10 days accumulation before sampling). No
296 significant relationships were observed between rainfall / estimated river flow and NH_3 .

300

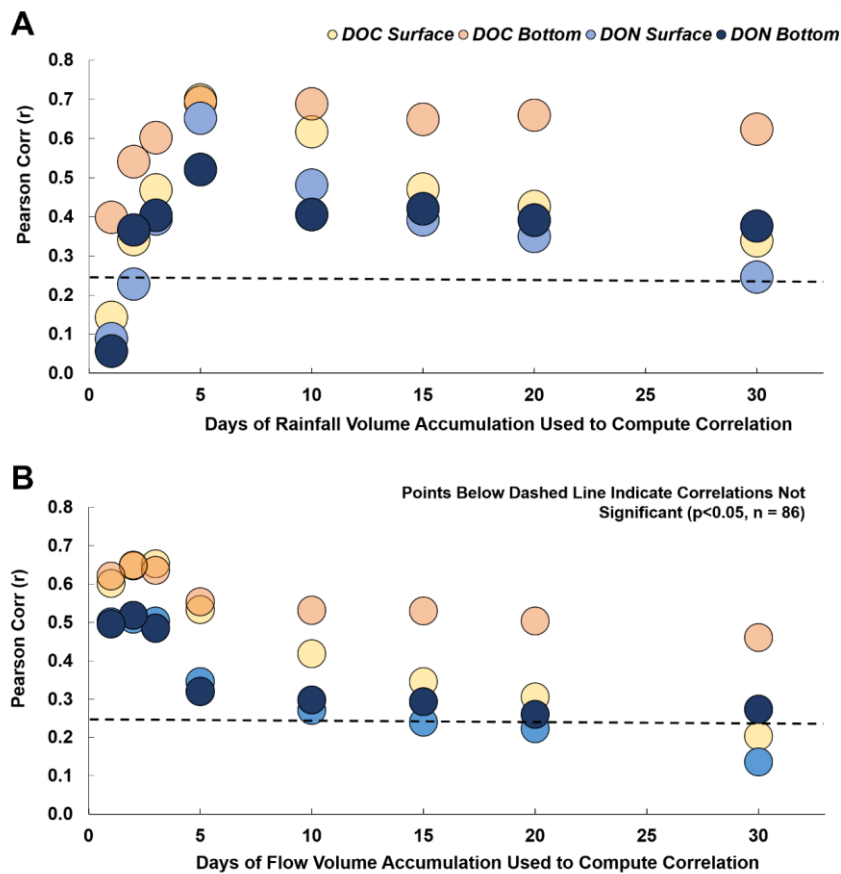
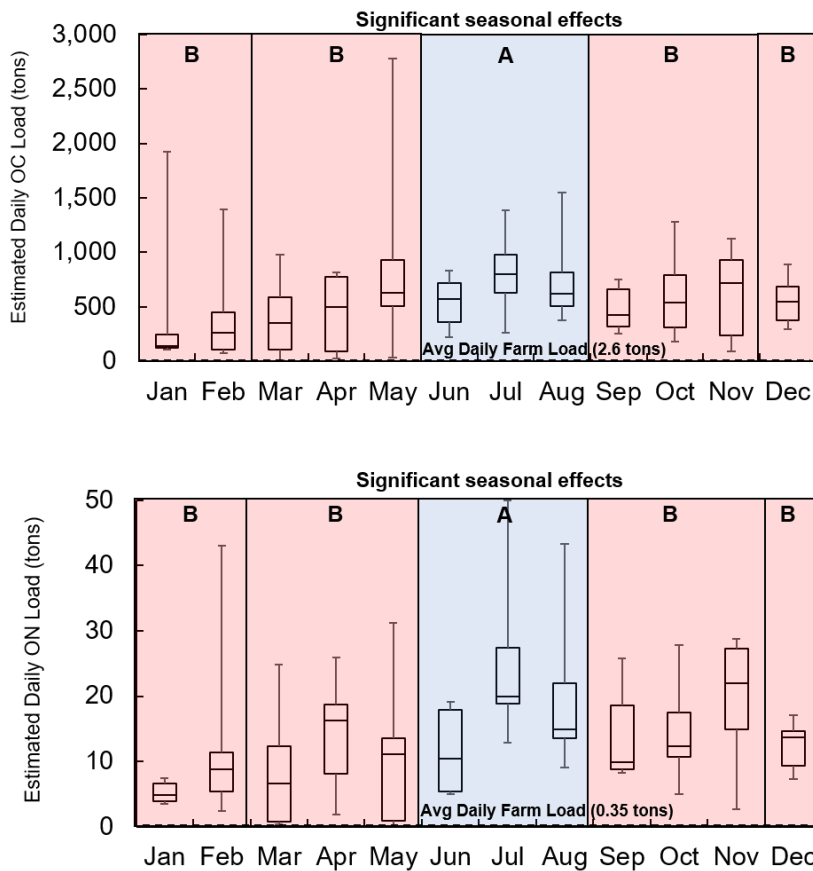


Figure 3: Pearson Correlation Coefficients (r) ($n = 86$) between dissolved organic C and dissolved organic N concentrations measured at the Gordon River mouth and (A) accumulated rainfall (B) accumulated flow at the Gordon River mouth. Note that all correlations are statistically significant ($p < 0.05$) except those circles whose centres are below the dashed line. The x-axis represents the number of days over which the volume of rain or estimated flow is summed and used to compute the correlations between DOC and DON. For instance, 5 days rainfall volume is equal to the rainfall volume measured at Strathgordon Gauge over the 5 days prior to water sampling at station GRI.

Two-way ANOVA (and subsequent Tukey HSD *post hoc* tests) revealed that DOC loading (calculated from samples collected at 2 m depths and 3-day flow accumulation) was observed to significantly ($p = 0.0478$) vary with season. Winter

Formatted: Font: Italic

(June to August) loadings (mean loading 642.8 ± 48.0 tons day⁻¹) were substantially-significantly greater than summer (December to February) loadings (mean loading 430.4 ± 57.8 tons day⁻¹) (Figure 4). The maximum OC loading rate was observed in May 2016 at 1,227 tons OC day⁻¹. Similar patterns and seasonal relationships were observed for ON loading.



315 Figure 4: Daily OC and ON loading (tons) for each month based on estimated daily flows and concentrations of OC and ON measured at the Gordon River mouth from 2015 to 2021. Note the large variation in the month of May is driven by large flows in years 2015 and 2016. Dashed line indicates average daily OC and ON loading from farm feed inputs based on 10,000 tonnes annual production, feed conversion rate = 1.3, assimilation rate of 85%, 49% feed carbon content, 6.7% feed nitrogen content. Post Hoc groupings show significantly higher loads in winter depicted as blue boxes (denoted group "A") relative to other seasons as red boxes denoted (group "B").

320

3.3 Dissolved Oxygen Distribution

Dissolved oxygen concentrations in Macquarie Harbour exhibited strong stratification and ranged from suboxic ($< 1\text{ mg L}^{-1}$) in the deep basins to over 10 mg L^{-1} at the surface (**Figure 5**). Below the surface lens of well-oxygenated water, there was a mixing zone of approximately 10 m where DO concentrations rapidly declined, and salinity increased. Consequently, the waters below the mixing zone (referred to as basin water) were more saline and DO poor than the surface waters.

Harbour basin waters closest to the ocean endmember generally had higher DO concentrations (*i.e.* means of approximately 4 mg L^{-1} observed at stations KR1 and C10; **Figures 5 and 6**). Towards the Gordon River, basin water DO concentrations were lower and were more often observed to be hypoxic ($< 2\text{ mg L}^{-1}$) or suboxic ($< 1\text{ mg L}^{-1}$). At stations near the ocean endmember (also the Harbour's deepest basins; C10 and C08), the DO concentration and salinity were often observed to increase with depth. This water mass is the product of DWR (see Hartstein *et al.*, 2019).

Our box model of Harbour basin waters indicates there is often hypoxic ($< 2\text{ mg L}^{-1}$) water present in the system and prolonged periods of suboxia ($< 1\text{ mg L}^{-1}$) (**Figure 7**). The most prolonged period of sustained suboxia occurred from June 2015 to May 2017. The largest volume of suboxic water was observed in May 2014 at over $60 \times 10^6\text{ m}^3$. The frequency of hypoxic and suboxic observations at any one station increased with proximity to the Gordon River mouth. For example, while station C10 experienced suboxia 13.8% of the time (of 96 months), station WH2 experienced suboxic conditions in nearly 37% of observations (of 120 months; **Figure 6**).

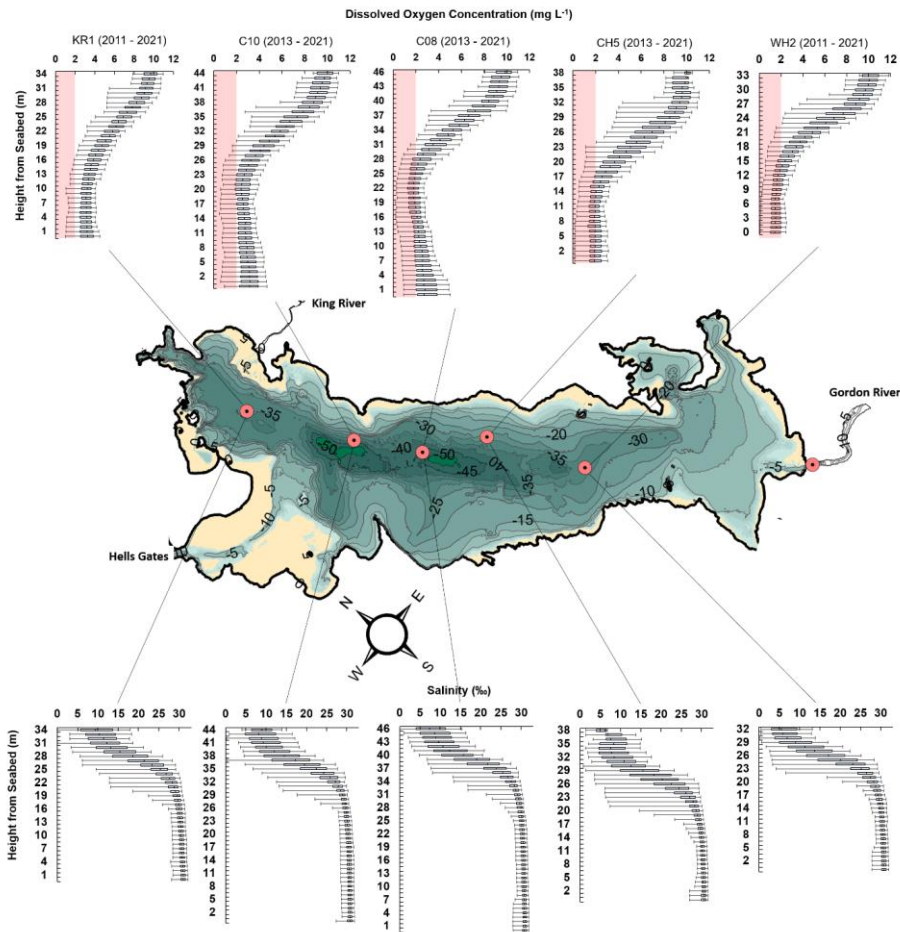


Figure 5: Box plots of dissolved oxygen concentration (mg L^{-1}) and salinity monthly profiles. Extent of dataset for each site is specified above the plots. Note vertical resolution is 1 m and references height from the seabed. Hypoxic ($< 2 \text{ mg L}^{-1}$) conditions are highlighted in red.

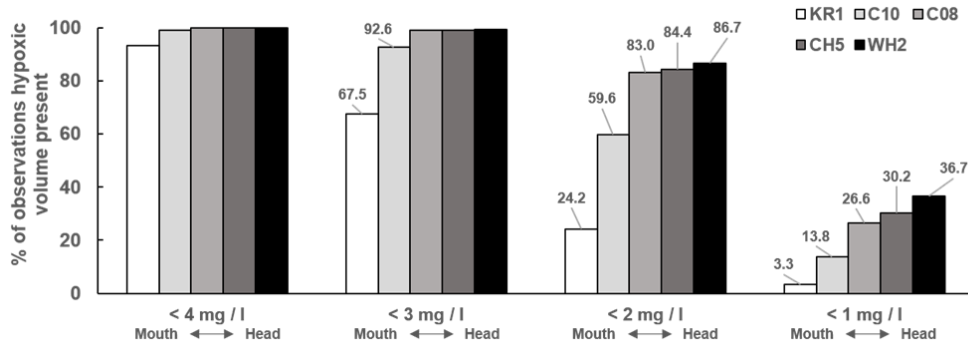


Figure 6: Percentage of total observations where monthly sonde profiles contained dissolved oxygen measurements less than 4 mg L⁻¹, 3 mg L⁻¹, hypoxic water (<2 mg L⁻¹), and suboxic (<1 mg L⁻¹) water at any depth.

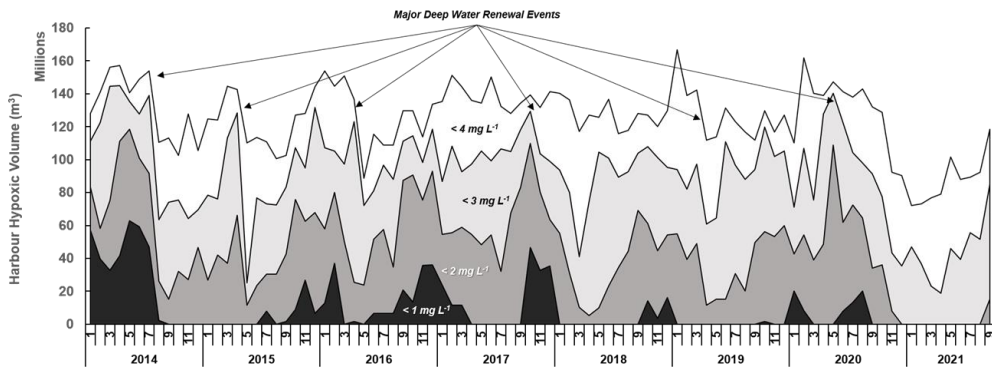


Figure 7: Estimated hypoxic volume present in the Harbour from 2014 to 2021, based on our 1 m resolution box model. Deep water renewal events are denoted by black arrows.

3.4 Rainfall and Dissolved Oxygen

There were significant correlations between rainfall and DO concentration along the entire Harbour longitudinal axis (Figure 8). However, the correlation's strength, significance, and direction varied with depth.

In the surface waters and through the mixing zone, the correlation between rainfall and DO concentration was positive (increased rainfall was observed with increased DO concentrations) and waned with depth ($r = 0.6$ 6m to 8 m below the surface at stations KR1, C10, and C08) (**Figure 8**). Towards the Gordon River at station WH2, the strongest correlation ($r = 0.677$, $p = 2 \times 10^{-17}$) was observed at approximately 10 m depth with the rainfall metric "20 days rain accumulation". At all stations, the strength of the correlation between rainfall and DO concentration decreased through the mixing zone, eventually to non-significance and no relationship. Approximately 30 m below the surface, the correlation (though not statistically significant) was observed to become inversely related to rainfall at all stations (more rainfall was observed with lower DO concentrations closer to the seabed).

365

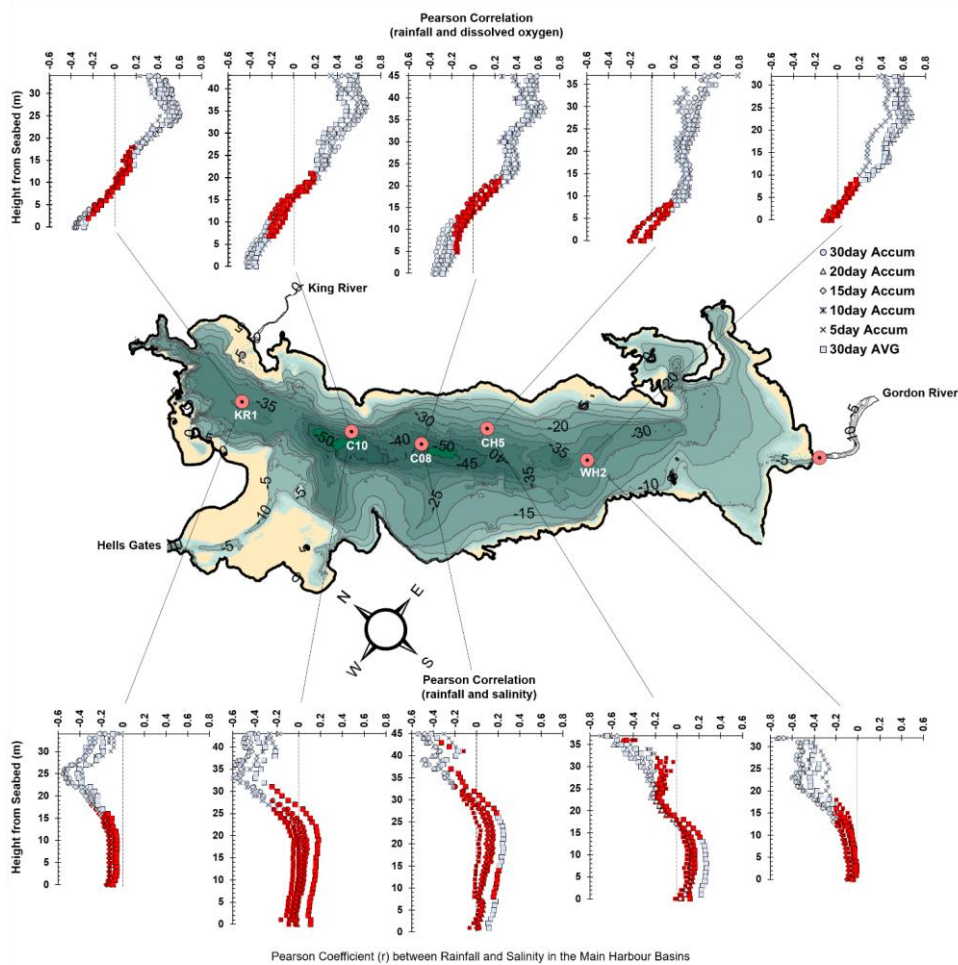
At stations whose monthly profiles extend into DWR waters (*i.e.* KR1, C10, C08), the relationship between rainfall and DO concentration strengthened and became statistically significant, though inversely related (high rainfall observed with low DO concentrations), with depth (**Figure 8**). The strongest correlation along the seabed ($r = -0.4238$, $p = 2.3 \times 10^{-5}$) was observed using 20-day rainfall accumulation at station C10, 3 m from the seabed. At station C08 the strongest correlation ($r = -0.3637$, $p = 0.00034$) in the basin was observed using 30-day rainfall accumulation, 1 m from the seabed.

370

3.5 Rainfall and Salinity

As observed in rainfall-DO relationships, there were significant correlations between rainfall and salinity, whose strength, significance, and direction varied with depth. There were significant inverse relationships between rainfall and salinity (*i.e.* more rainfall associated with lower salinity) that reached a maximum strength ($r = -0.6$) 10 m below the surface for stations near the ocean endmember. In shallow water, these relationships became stronger (r is observed to approach 0.8 at CH5) closer to the Gordon River (**Figure 8**). The relationship between rainfall and salinity rapidly weakened in the mixing zone to statistical insignificance.

375



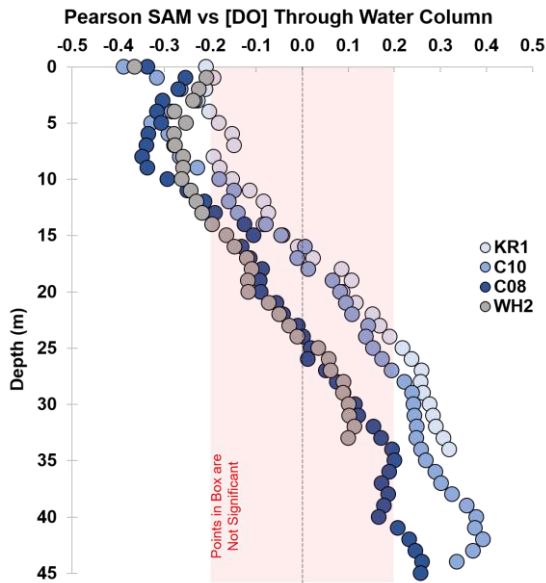
380

Figure 8: Pearson correlation coefficients (r) between rainfall and dissolved oxygen (top) and rainfall and salinity (bottom) through the water column at 1m vertical resolution. Selected rainfall metrics include accumulation 30 days prior to sampling (circles), 20 days (triangles), 15 days (diamonds), 10 days (asterisk), and 5 day (x) accumulation, and 30 day average daily rainfall prior to sampling (squares). Red symbols denote statistical insignificant correlations ($p < 0.05$). Vertical dashed lines represent $r = 0$.

385

3.5 Southern Annular Mode and Dissolved Oxygen

There were depth specific statistically significant Pearson correlations between monthly SAM index values and DO concentration at each sampling station (Figure 9). In the surface waters the correlations were negative and became increasingly more positive with depth. The strongest relationships in the surface waters occurred at stations closest to the mouth of the Harbour (except for station KR1, nearest the King River mouth). The strength of the correlations weakened with depth and eventually displayed positive r values (indicating the opposite relationship). The DO at stations nearest the sill responded most strongly to SAM index values along the seabed, with statistically significant positive correlations (high SAM index associated with higher DO concentration) observed at stations C10, C08, and KR1.



395 **Figure 9:** Pearson correlation coefficients (r) between Southern Annular Mode (SAM) Index and dissolved oxygen concentrations at KR1, C10, C08, and WH2 through the water column at 1m vertical resolution. Red box denotes statistical insignificant correlations while all points outside of the box indicate statistically significant correlations ($p < 0.05$). Note points reference water depth not height off seabed.

4 Discussion

400 4.1 Rainfall, Oxygen Distribution, and Implications for Green House Gas Production

The water column structure in Macquarie Harbour is similar to that of many fjord and fjord-like DCIs distributed throughout the world's mid to high latitude coastlines. The sill at the system's mouth sets up a strongly stratified water column isolating basin water from the surface (Inall and Gillibrand, 2011; Calvete and Sobarzo, 2011). The largest freshwater source, the Gordon River, discharges dissolved organic carbon loads (often over 500 tonnes per day; **Figure 4**; also see **Appendix**
405 **Figures A1** and **A2** for context) limiting light penetration to within the first few meters of the water column. These loads restrict photosynthesis in the system to the surface layer (demonstrated by rapidly attenuated chlorophyll-*a* with surface concentrations of 4 to 5 $\mu\text{g L}^{-1}$ and generally undetectable levels at 12 m; see **Appendix Figure A3**).

OC and ON loading exhibited seasonality with significantly greater loadings in winter compared to summer (**Figure 4**).
410 These loads are products of both greater flow volume and significant increases in the measured concentration of OC and ON (**Figure 3**).

The lack of light penetration coupled with limited basin water exchange and large riverine OM loads makes the subsurface waters of this system, and many other similar fjord-like DCIs, naturally prone to oxygen-poor conditions (see Gonsior *et al.*, 2008; Bianchi *et al.*, 2020). The distribution of dissolved oxygen in Macquarie Harbour is closely tied to the
415 physical separation of the water masses. DO is greatest in surface waters near system endmembers (**Figure 5**), while hypoxia forms regularly and with varying intensity for extended periods in its basins. Below the freshwater lens, $\text{DO} < 4 \text{ mg L}^{-1}$ occurs in >90% of observations and hypoxia ($< 2 \text{ mg L}^{-1}$) was observed more than 80% of the time (stations C08 towards WH2; **Figure 6**). Suboxic ($< 1 \text{ mg L}^{-1}$) concentrations are observed at every station, but more often (up to 36% of the time)
420 at stations closest to the Gordon River. Suboxic conditions have persisted for up to 2 years (**Figure 7**).

The primary mechanism by which basin water is re-oxygenated is the intrusion of ocean water over the sill (*i.e.* DWR). DWR occurs regularly (see Hartstein *et al.*, 2019) but according to our analysis only 5 to 7 times per decade for volumes significant enough to relieve suboxic conditions up-harbour (see **Figure 7**). The drivers of DWR were examined in
425 Hartstein *et al.* (2019) and included sustained N and NW winds and low ($< 990 \text{ hPa}$) atmospheric pressure. One of the DWR drivers not entirely resolved was the role of freshwater inputs into the system. Our analysis of rainfall and DO distribution suggests that during periods of high rain (*i.e.* winter), DO tends to be lower just above the seabed (**Figure 8**). During periods of low rainfall (*i.e.* summer), DO above the seabed is higher. Correlations between rainfall and DO concentration were not statistically significant through a large portion of the sub-halocline, but with depth became
430 statistically significant a few meters above the seabed (see **Figure 8**). This depth-dependent relationship between rainfall and

DO suggests that the amount of river water entering the system is an important driver of DWR and thus the distribution of DO.

Our analysis shows that with increased rainfall, DOC and DON loading increases as a result of both increased river flow as well as increased concentrations of DOC and DON present in the water (Figure 3). The majority of the additional OM entering the system is primarily dissolved and likely retained in the surface lens where DO concentrations are at their highest. It is important to note that Macquarie Harbour is a “black water system” with relatively low chlorophyll-a concentrations at the surface and undetectable levels in the halocline (in this case 12m depth). The contribution of phytoplankton production to eutrophication would be limited by poor light availability. Undoubtedly some river-derived OM will reach the dark sub-halocline layers and depending on its lability will contribute to the removal of dissolved oxygen from the water column through respiratory processes. With increased rainfall riverine OM contributions to the basins could increase (increased eutrophication) thus increasing oxygen demand and decreasing the standing oxygen concentration. However, in a previous study (Maxey *et al.*, 2020) the effect of increased riverine OM loading on the rate of basin water column oxygen demand was not significant (although they only measured this process for 6 months), suggesting that much of the riverine OM is flushed outside of the system and / or is mostly refractory material. ▲

Formatted: Font: Bold

Formatted: Font: Not Bold

Rainfall in the Macquarie Harbour catchment is influenced by the oscillations of the Southern Annular Mode (SAM). Our analysis also showed that SAM index values significantly correlated with DO conditions in the surface and near-bottom layers. Positive SAM index values were associated with lower DO in the surface waters and higher oxygen concentrations in the basins nearest the sill (Figure 9). Positive SAM index values indicate high pressure in the southern hemisphere mid-latitudes, leading to weaker westerly winds (Taschetto and England, 2009; Dey *et al.*, 2018). For the West Coast of Tasmania, weaker westerly winds result in less moisture captured by the mountain ranges that form the eastern edge of the Harbour’s catchment and subsequently, less rainfall occurs. Less rainfall in the catchment means less river flow to the Harbour, which promotes DWR and relieves deep basin hypoxia. Austin and Inall (2002) observed similar broad-scale climate oscillations (in this case, the North Atlantic Oscillation) affecting the basin water in Scottish Sea Lochs.

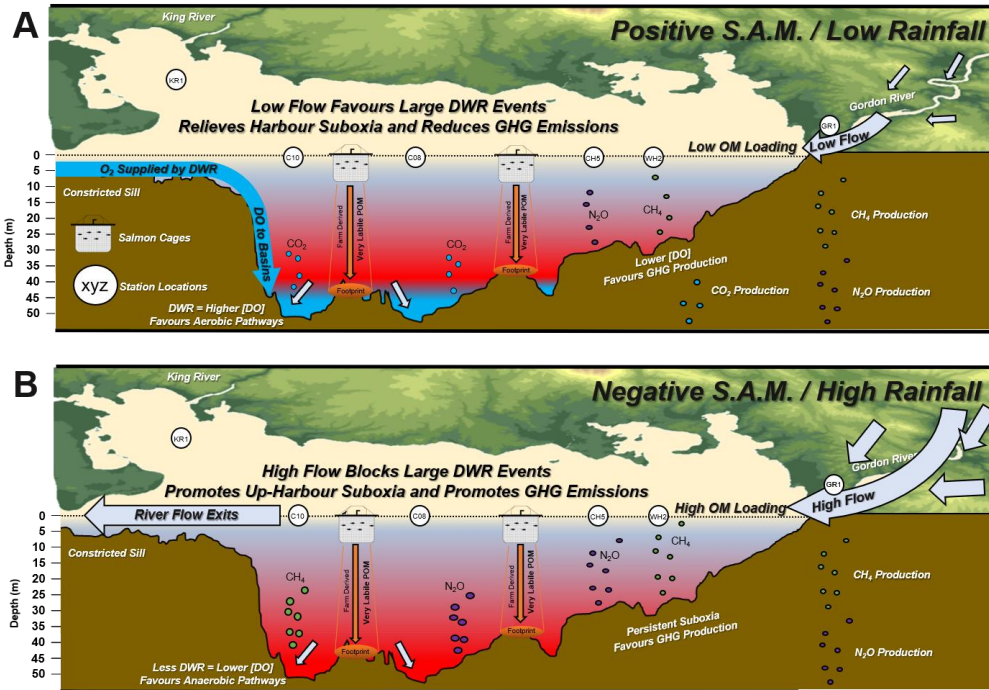
Rainfall metrics and the effect of SAM only significantly correlated with surface waters and the deeper basin waters of the Harbour (Figures 8 and 9). Without a direct supply of oxygen from either physical mixing or photosynthesis, the slow but steady uptake of DO by microbes (into heterotrophic (*e.g.* aerobic respiration) and autotrophic (*e.g.* ammonia oxidation) pathways establishes oxygen-poor conditions (Maxey *et al.*, 2020). The low light and suboxic conditions often present in the sub-halocline up Harbour likely promote DO uptake by nitrifying microbes. Depending on the amount of available DO, the eventual end product of ammonia oxidation (first step of nitrification) may differ (Arrigo, 2005; Codispoti *et al.*, 2005; Lam *et al.*, 2011). At suboxic concentrations, ammonia oxidation begins to favour the production of N₂O (a potent greenhouse gas; GHG) over NO₂⁻ (Goreau *et al.*, 1980; Ji *et al.*, 2018; Frey *et al.*, 2020). Da Silva *et al.*, (2021) observed significant differences in the microbial communities present in the Harbour’s basin waters, with

465 communities comprising a more significant proportion of GHG producers than in the surface waters. Our improved
 understanding of the drivers and oxygen distribution in the system seems to corroborate their findings. Their observations of
 community composition and our DO distribution observations in the Harbour suggest that the basins' communities are
 primed for GHG production during periods of prolonged suboxia.

470

The eventual fate of riverine OC and ON entering the harbours basins will depend upon the oxygen conditions present.
 Suboxic DO conditions favour the production of GHG such as CH₄ and N₂O, and the lack of large DWR events promotes
 suboxic basin water conditions. High freshwater inputs are associated with low basin water DO, and we postulate that this is
 due to the impediment of DWR. In Macquarie Harbour and DCIs with constricted inlets and large rivers, the physical effects
 475 of rainfall or river flow (as driven by broader climate forcings like SAM) may be tied to the eventual fate of C and N
 entering the system (**Figure 10**).

Formatted: Font: Not Bold



480 **Figure 10: Conceptualisation of the role of freshwater inputs on the distribution of DO and potential for GHG production in the Harbour. (A) Harbour DO and GHG during periods of low rainfall (or positive SAM index) promoting DWR. (B) High rainfall (negative SAM index) blocks DWR and promotes the spread of suboxia and thus GHG production.**

4.2 Climate Change Predictions for Tasmania's West Coast and Dissolved Oxygen

485 Climate change predictions for the west coast of Tasmania suggest that there will be greater and more intense rainfall in the winter and lower rainfall in summer (Viney *et al. et al.*, 2009; Grose *et al. et al.*, 2010; Bennett *et al. et al.*, 2010). Increased rainfall means greater river flow and OM loading (Figures 2 and 3) and is associated with decreased basin water DO in this system (Figure 8). High winter river flow may reduce the chances of significant DWR events and promote prolonged basin water suboxia [by stimulating pelagic oxygen demand through increased riverine OM loading \(Maxey et al., 2020; Figure 10\)](#).

490 While large DWR events have occurred during both summer and winter, they are infrequent (*see* Hartstein *et al. et al.*, 2019). Increased winter river flow may reduce the chance of DWR occurrence by blocking marine intrusions over the sill; this would result in more extended periods of basin water suboxia and GHG production. An analysis of the weather station wind data available from 1993 to 2014 at Cape Sorell (near Hell's Gates Inlet; *see* Figure 1 for location) shows that wind conditions required for DWR (sustained N and NW winds; Hartstein *et al. et al.*, 2019) are more frequent (over 30% of the time) in winter compared to summer (18% of occurrences). If the climate predictions discussed in Grose *et al. et al.*, (2010) and Bennett *et al. et al.*, (2010) are realised, then this may result in a disproportionate reduction in significant DWR events for the Harbour and increased GHG emissions. Likewise, if winter rainfall is reduced, DWR may become disproportionately more frequent, thus reducing potential GHG emissions.

500 It is the orientation of Macquarie Harbour that makes N and NW winds a significant driver of DWR. Sustained winds from this direction push water up the Harbour's longitudinal axis, creating wind set up at the head of the system, and obliges marine water to cross the sill (Hartstein *et al. et al.*, 2019). Upon entering the main harbour body, the oxygen rich dense marine water mass sinks into the deepest basins. If climate change affects the frequency and duration of wind occurring in N and NW directions, DWR (and GHG emissions) may be affected through an additional mechanism independent of rainfall (e.g. changes in wind direction).

510 There is some evidence that climate forcings (like SAM) have been significantly strengthening winds and waves along Tasmania's west coast since the 1970s (*see* Hemer, 2010a and 2010b; Kirkpatrick *et al. et al.*, 2017; Marshall *et al. et al.*, 2018; Sharples *et al. et al.*, 2020). If climate driven increases in wind speed result in changes to the N and NW wind patterns, then this may have implications for DWR frequency in the Harbour. Likewise, increased wind and wave forcings have been

suggested as a cause for further sedimentation of the harbour mouth (Sharples *et al.*, 2020), which would constrict the sill and impede DWR. At the moment, the confluence of large-scale climate drivers (*e.g.* increasing SAM; climate driven winds and rainfall patterns) make predicting future DWR patterns (and the resulting GHG release) in Macquarie Harbour a difficult task.

515

In other fjord and fjord-like DCIs, the predicted impact of climate change on rainfall varies, as does each system's sensitivity to freshwater input for DWR. In scenarios where freshwater input is the important driver of bottom-water oxygenation (for instance, Lochs Etive (in Edwards & Edelsten, 1977; Austin and Inall, 2002; Gillibrand *et al.*, 1995) and Ailort (in Gillibrand *et al.*, 1996) increased freshwater supply may increase the extent and duration of hypoxia and thus GHG emissions. Less frequent DWR may be further exacerbated by coastal deoxygenation (see Keeling *et al.*, 2010; Levin and Breitburg, 2015; Wang *et al.*, 2017; Gupta *et al.*, 2021). In such systems with coastal deoxygenation, the oxygen mass introduced to basins will be lower, further promoting hypoxia and potential GHG release.

520

One of the critical factors buffering GHG releases from these systems is the well-oxygenated surface water layer. Some portion of the dissolved CH₄ produced in sediments and suboxic regions of the Harbour might be oxidised upon reaching more normoxic regions (Reeburgh, 2007). In many systems the relatively high concentrations of CH₄ produced in deeper anoxic portions of the system are observed to be reduced in surface layers (*e.g.* Storfjorden in Mau *et al.*, 2013; Pearl River Estuary in Ye *et al.*, 2019; Saguenay Fjord in Li *et al.*, 2021). Nevertheless, the concentration of CH₄ at the surface can often be observed at supersaturated concentrations and thus will still be sources of CH₄ to the atmosphere. The ebullition of GHG produced in sediments can also shuttle CH₄ to the surface before it is fully oxidised. This process is heavily influenced by physical factors such as sediment grain size (higher magnitudes in finer sediments) and hydrostatic pressure (Liu *et al.*, 2016; De Mello NAST *et al.*, 2018). In Macquarie Harbour, and many DCIs, the areas most prone to suboxia are areas where the underlying seabed is composed of fine-grained organic-rich riverine sediment (Carpenter *et al.*, 1991; Teasdale *et al.*, 2003). Additionally, the water level (and thus hydrostatic head) in the Harbour and many other systems varies with freshwater supply and would also contribute to the ebullition of CH₄.

525

530

535

Whether the magnitude of climate-induced GHG emissions from DCIs are significant enough to accelerate further climate change (and thus further accelerate GHG emissions through a positive feedback loop) (**Figure 10**) remains to be seen. While the oceanographic mechanisms by which fjord-like DCIs operate are similar, their unique morphologies and surrounding landscapes / hydrologies must be better understood to account for their potential as sources of GHG under future climate scenarios. In order to better manage resource use affecting these systems (*e.g.* hydroelectric dams, salmon farms, discharge outfalls), understanding the connection between the physical processes (such as freshwater supply, weather patterns, DWR) and biogeochemical processes (pelagic oxygen demand, CH₄ and N₂O production, CH₄ oxidation) needs to be established.

540

Formatted: Font: Not Italic

545 4.3 Harbour Management Implications

Resource use in Macquarie Harbour is similar to that of many DCIs. The relatively deep, cool, and oxygen-rich sheltered waters provide an excellent location for sea cage salmon aquaculture (Gillibrand and Turrell, 1997; Skogen *et al.*, 2009; Inall and Gillibrand, 2010). Sea cage culture requires the fish to be immersed in their environment, and in Macquarie Harbour the areas where farms are situated span some of the area over the deepest basins (**Figure 1**). Significant DWR events, like those occurring in May 2015, can cause physical disturbances to water column structure (*e.g.* internal waves) that significantly affect fish farms. The May 2015 event, for example, caused internal waves that transported oxygen-poor bottom water to the surface (Hartstein *et al.*, 2019). Because rainfall affects DWR, the predicted increase in winter intensity may reduce the chances of significant DWR events and thus reduce the likelihood of adverse physical disturbances to fish farms. On the negative side, farm-derived feed and faeces waste represent a highly labile source of OM to the seabed.

555

Farm waste footprints may be hotspots of GHG production, but the magnitude of that production is still largely undescribed. If climate change reduces the frequency of DWR, the processing of farm-derived OM may be less efficient as less oxygen will be available to fuel aerobic respiration (Brooks *et al.*, 2000; Hartstein, 2003; Pereira *et al.*, 2004). This may lead to possible increased GHG production and will facilitate the spread of *Beggiatoa* matting (Crawford *et al.*, 2001; Crawford, 2003). Presently, no studies describe the rate of the GHG output under salmon farms in any of these systems, leaving open a significant knowledge gap for future aquaculture and GHG research.

560

Rainfall is not the only driver of river flow into the Harbour. The Macquarie Harbour catchment has two upstream hydroelectric dams regulating flow into the main rivers. Dam release water introduces additional POC and DOC load, especially during low reservoir periods (MHDOWG, 2014). These releases may impact DWR by blocking events that might otherwise have occurred. Given the infrequency of large DWR events and their important role in mitigating basin water suboxia, it seems prudent for hydroelectric management to consider the implications of ill-timed releases on harbour health and their subsequent impacts on GHG production.

565

570 5 Conclusions

In summary, rainfall significantly affects OM and nutrient concentrations entering Macquarie Harbour. Importantly, rainfall is seasonal and has a significant depth specific impact on the distribution of dissolved oxygen in the harbour body. It appears that the impact of rainfall on basin water hypoxia is driven by physical forcings, namely the impediment of DWR.

575

The Southern Annular Mode (SAM) climate oscillation index also significantly correlates with DO concentrations in the surface layer and a few meters above the seabed. However, the direction of the correlation is layer-specific. The SAM index

is highly variable but has been increasing in recent decades. Climate change is predicted to result in wetter winter / drier summers for the Tasmanian West Coast, resulting in fewer DWR events in winter and more frequent and intense DWR events in summer.

580

Currently, there is no information describing the distribution of CH₄ and N₂O in Macquarie Harbour or how this varies with river loading. However, the DO distribution suggests that most of the production will be near the Gordon River mouth (*e.g.* stations CH5 and WH2). If DWR is stymied in winter by increased rainfall, the suboxic conditions promoting GHG production may become even more prolonged, especially up-harbour.

585

6 Appendices

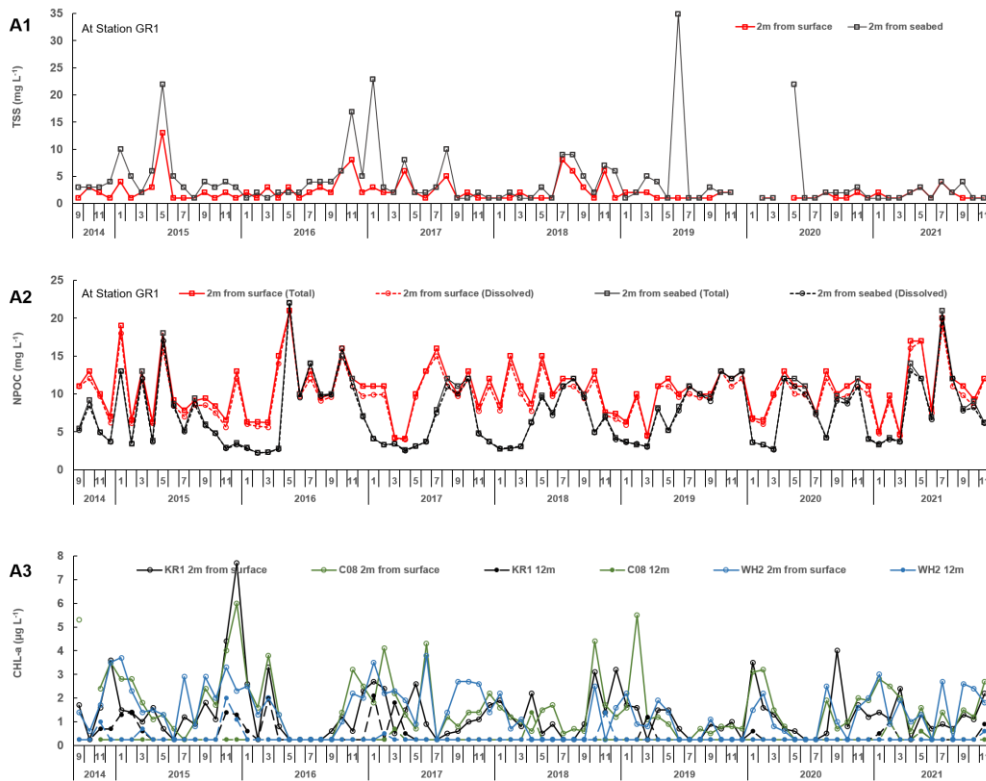


Figure for Appendix: (A1) Total Suspended Solids concentrations observed at station GR1. Samples collected 2m from surface (red) and 2m from seabed (black). (A2) Total organic carbon (solid lines) and dissolved organic carbon (dashed lines) concentrations observed at station GR1. Samples collected 2m from surface (red) and 2m from seabed (black). (A3) Chlorophyll-a collected from stations KR1 (black), C08 (green), and WH2 (blue). Samples collected 2m from surface (solid lines open symbols) and 12m from surface (dashed lines closed symbols). All data displayed reflect dates from September 2014 to November 2021 and are used here as an example of Macquarie Harbour water column properties.

7 Data Availability

This data set is not available for the public.

600 8 Author Contributions

Johnathan Daniel Maxey – *Conceptualization, Field Collection, Analytical Methodology, Data Analysis, Writing – Original Draft, Writing – Review & Editing*

605 **Neil David Hartstein** – *Conceptualization, Field Collection, Analytical Guidance, Writing – Review & Editing, Funding*

Aazani Mujahid – *Writing – Review & Editing*

610 **Moritz Müller** – *Analytical Guidance, Writing – Review & Editing, Funding*

9 Acknowledgements

We would like to thank the Analytical Services Tasmania for their help in clarifying methods descriptions and general discussions about the implications of analytical methods. Appreciation to Hydro Tasmania and the Bureau of Meteorology for providing links to rainfall and river flow data within the Gordon River catchment. We want to thank the vessel operators for their tireless efforts during the many inclement weather days spent with us on the Harbour (Sam and Sean Gerrity, the late Trevor Dennis, Torsten Schwoch, and Ryan Gunton) and the many technicians responsible for helping to collect portions of this field dataset (Justyn, Dora, Grace, Shukry, Amirul). We would also like to thank our families for supporting those long days away from home and hours spent in front of the screen to get this information and its implications published - we had to borrow the time from you, and we are grateful. This research has been supported by the Newton-Ungku Omar Fund (grant no. NE/P020283/1).

615
620

10 Competing Interests

The authors declare that they have no conflict of interest.

11 References

- 625 Arrigo, K. R.: ~~(2005)~~ Marine microorganisms and global nutrient cycles. *Nature*, 437(7057), 349-355. ~~(2005)~~.
- 630 Augustinus, P., Barton, C. E., Zawadzki, A., & Harle, K.: ~~(2010)~~ Lithological and geochemical record of mining-induced changes in sediments from Macquarie Harbour, southwest Tasmania, Australia. *Environmental Earth Sciences*, 61(3), 625-639. ~~(2010)~~.
- 630 Austin, W. E., & Inall, M. E.: ~~(2002)~~ Deep-water renewal in a Scottish fjord: temperature, salinity and oxygen isotopes. *Polar Research*, 21(2), 251-257. ~~2002~~.
[Austin and Inall 2011](#)
- 635 Baker, W. E., & Ahmad, N.: ~~(1959)~~ Re-examination of the fjord theory of Port Davey, Tasmania. In *Papers and Proceedings of the Royal Society of Tasmania*. (Vol. 93, pp. 113-116). ~~1959~~.
- 640 Bennett, J. C., Ling, F. L. N., Graham, B., Grose, M. R., Corney, S. P., White, C. J., Holz, G. K., Post, D. A., Gaynor, S. M. and Bindoff, N. L.: ~~2010~~, Climate Futures for Tasmania: water and catchments technical report, Antarctic Climate & Ecosystems Cooperative Research Centre, Hobart, Tasmania., ~~2010~~.
- Bianchi, T. S., Cui, X., Blair, N. E., Burdige, D. J., Eglinton, T. I., & Galy, V.: ~~(2018)~~ Centers of organic carbon burial and oxidation at the land-ocean interface. *Organic Geochemistry*, 115, 138-155. ~~2018~~.
- 645 Bianchi, T. S., Arndt, S., Austin, W. E., Benn, D. I., Bertrand, S., Cui, X., Faust, J., Kozirowska-Makuch, K., Moy, C., Savage, C., Smeaton, C., Smith, R., & Syvitski, J.: ~~(2020)~~ Fjords as aquatic critical zones (ACZs). *Earth-Science Reviews*, 203, 103145. ~~2020~~.
- 650 Breitburg, D., Levin, L. A., Oschlies, A., Grégoire, M., Chavez, F. P., Conley, D. J., Garçon, V., Gilbert, D., Gutiérrez, D., Isensee, K. and Jacinto, G. S.: ~~(2018)~~ Declining oxygen in the global ocean and coastal waters. *Science*, 359(6371). ~~2018~~.
- Brooks, K.M.: ~~2000~~ Salmon Farm Benthic and Shellfish Effects Study 1996–1997. *Aquatic Environmental Sciences*, 644 Old Eaglemount Road, Port Townsend, WA 98368. 117 pp. ~~2000~~

655 Cage, A. G. ~~(2006)~~; The modern and late Holocene marine environments of Loch Sunart, NW Scotland. ~~(Doctoral~~
dissertation, University of St Andrews. 2006.

Calvete, C., & Sobarzo, M. ~~(2011)~~; Quantification of the surface brackish water layer and frontal zones in southern Chilean
fjords between Boca del Guafo (43 30' S) and Estero Elefantes (46 30' S). Continental Shelf Research, 31(3-4), 162-171.
660 2011.

Carpenter, P. D., Butler, E. C. V., Higgins, H. W., Mackey, D. J., & Nichols, P. D. ~~(1991)~~; Chemistry of trace elements,
humic substances and sedimentary organic matter in Macquarie Harbour, Tasmania. Marine and Freshwater Research,
42(6), 625-654. 1991.

665 Codispoti, L. A., Yoshinari, T., & Devol, A. H. ~~(2005)~~; Suboxic respiration in the oceanic water column. in: Respiration in
Aquatic Ecosystems, edited by: del Giorgio, P., and Williams, P., Oxford University Press, 225-247.
DOI:10.1093/acprof:oso/9780198527084.001.0001, 2005.

670 Cracknell, M. J., Nascimento, S. C., Heng, W. X., Parbhakar-Fox, A., & Schaap, T. A. ~~(2019)~~; Geophysical investigation of
mine waste in the King River Delta, Macquarie Harbour, Tasmania. ASEG Extended Abstracts, 2019(1), 1-4. 2019

Crawford, C. M., Mitchell, I. M., & Macleod, C. K. A. ~~(2001)~~; Video assessment of environmental impacts of salmon
farms. ICES Journal of Marine Science, 58(2), 445-452. 2001.

675 Crawford, C. ~~(2003)~~; Environmental management of marine aquaculture in Tasmania, Australia. Aquaculture, 226(1-4),
129-138. 2003.

Cresswell, G. R., Edwards, R. J., & Barker, B. A. ~~(1989)~~; Macquarie Harbour, Tasmania-seasonal oceanographic surveys in
680 1985. In Papers and Proceedings of the Royal Society of Tasmania, (v)Vol. 123, pp-63-66. 1989.

Da Silva, R. R. P., White, C. A., Bowman, J. P., Raes, E., Bisset, A., Chapman, C., Bodrossy, L. and Ross, D.J. ~~(2021)~~;
Environmental influences shaping microbial communities in a low oxygen, highly stratified marine embayment. Aquatic
Microbial Ecology, 87, pp-185-203. 2021.

685 de Mello, N. A. S. T., Brighenti, L. S., Barbosa, F. A. R., Staehr, P. A., & Bezerra Neto, J. F. ~~(2018)~~; Spatial variability of
methane (CH₄) ebullition in a tropical hypereutrophic reservoir: silted areas as a bubble hot spot. Lake and Reservoir
Management, 34(2), 105-114. 2018.

Formatted: Subscript

- 690 del Giorgio, P., & Williams, P. (Eds.). ~~(2005)~~. Respiration in aquatic ecosystems. [Oxford University Press](#).
[DOI:10.1093/acprof:oso/9780198527084.001.0001, 2005](#)
~~OUP Oxford.~~
- 695 Dey, R., Lewis, S. C., Arblaster, J. M., & Abram, N. J. ~~(2019)~~. A review of past and projected changes in Australia's
rainfall. [Wiley Interdisciplinary Reviews: Climate Change](#), 10(3), e577, [2019](#).
- Diaz, R. J., & Rosenberg, R. ~~(2008)~~. Spreading dead zones and consequences for marine ecosystems. [Science](#), 321(5891),
926-929, [2008](#).
- 700 Edgar, G. J., Barrett, N. S., & Last, P. R. ~~(1999)~~. The distribution of macroinvertebrates and fishes in Tasmanian estuaries. [Journal of Biogeography](#), 26(6), 1169-1189, [1999](#).
- Edwards, A., & Edelsten, D. J. ~~(1977)~~. Deep water renewal of Loch Etive: a three basin Scottish fjord. [Estuarine and Coastal Marine Science](#), 5(5), 575-595, [1977](#).
- 705 Eriksen, R. S., Mackey, D. J., van Dam, R., & Nowak, B. ~~(2001)~~. Copper speciation and toxicity in Macquarie Harbour,
Tasmania: an investigation using a copper ion selective electrode. [Marine Chemistry](#), 74(2-3), 99-113, [2001](#).
- 710 Featherstone, A. M., & O'grady, B. V. ~~(1997)~~. Removal of dissolved copper and iron at the freshwater-saltwater interface of
an acid mine stream. [Marine Pollution Bulletin](#), 34(5), 332-337, [1997](#).
- Fogt, R. L., & Marshall, G. J. ~~(2020)~~. The Southern annular mode: Variability, trends, and climate impacts across the
Southern Hemisphere. [Wiley Interdisciplinary Reviews: Climate Change](#), 11(4), e652, [2020](#).
- 715 Frey, C., Bange, H. W., Achterberg, E. P., Jayakumar, A., Löscher, C. R., Arévalo-Martínez, D. L., León-Palmero, E., Sun,
M., Sun, X., Xie, R. C. and Oleynik, S. ~~(2020)~~. Regulation of nitrous oxide production in low-oxygen waters off the coast of
Peru. [Biogeosciences](#), 17(8), pp.2263-2287, [2020](#).
- 720 Gade, H. G., & Edwards, A. ~~(1980)~~. Deep water renewal in fjords. In [Fjord oceanography](#), edited by: [Freeland, H. J. D. M.](#)
[Farmer, C. D. Levings](#). (pp. 453-489). Springer, Boston, MA, 453-489, ISBN: 978-1-4613-3107-0, 1980.

Geyer, W. R., & Cannon, G. A.: ~~(1982)~~ Sill processes related to deep water renewal in a fjord. *Journal of Geophysical Research: Oceans*, 87(C10), 7985-7996. ~~(1982)~~.

725 Gilbert, D., Rabalais, N. N., Diaz, R. J., & Zhang, J.: ~~(2010)~~ Evidence for greater oxygen decline rates in the coastal ocean than in the open ocean. *Biogeosciences*, 7(7), 2283-2296, [2010](#).

~~Walinsky et al. 2009~~

Formatted: Highlight

730 Gillibrand, P. A., & Turrell, W. R.: ~~(1997)~~ The use of simple models in the regulation of the impact of fish farms on water quality in Scottish sea lochs. *Aquaculture*, 159(1-2), 33-46, [1997](#).

Gillibrand, P. A., Cage, A. G., & Austin, W. E.: ~~(2005)~~ A preliminary investigation of basin water response to climate forcing in a Scottish fjord: evaluating the influence of the NAO. *Continental Shelf Research*, 25(5-6), 571-587, [2005](#).

735 Gillibrand, P. A., Cromey, C. J., Black, K. D., Inall, M. E., & Gontarek, S. J.: ~~(2006, February)~~ Identifying the risk of deoxygenation in Scottish sea lochs with isolated deep water. In *Scottish Aquaculture Research Forum, SARF (Vol. 7)*, [2006a](#).

740 Gillibrand, P.A. and Inall, M.E., ~~(2006)~~ Improving Assimilative Capacity Modelling for Scottish Coastal Waters: I. A Model of Physical Exchange in Scottish Sea Lochs. *Marine Physics Report No 167*, Scottish Association for Marine Science, Oban, 25, [2006b](#), pp.

~~Austin and Inall 2011~~

Formatted: Highlight

745 Gonsior, M., Peake, B. M., Cooper, W. J., Jaffé, R., Young, H., Kahn, A. E., & Kowalczyk, P.: ~~(2008)~~ Spectral characterization of chromophoric dissolved organic matter (CDOM) in a fjord (Doubtful Sound, New Zealand). *Aquatic Sciences*, 70(4), 397-409, [2008](#).

750 Goreau, T. J., Kaplan, W. A., Wofsy, S. C., McElroy, M. B., Valois, F. W., & Watson, S. W.: ~~(1980)~~ Production of NO₂- and N₂O by nitrifying bacteria at reduced concentrations of oxygen. *Applied and Environmental Microbiology*, 40(3), 526-532, [1980](#).

Formatted: Subscript

Formatted: Subscript

755 Goyal, R., England, M. H., Jucker, M., & Sen Gupta, A.: ~~(2021)~~ Response of Southern Hemisphere western boundary current regions to future zonally symmetric and asymmetric atmospheric changes. *Journal of Geophysical Research: Oceans*, 126(11), e2021JC017858, [2021](#).

Grose, M. R., Barnes-Keoghan, I., Corney S. P., White -C. J., Holz, G. K., Bennett, J. B., Gaynor, S. M. and Bindof, N. L.: ~~(2010)~~, Climate Futures for Tasmania: general climate impacts technical report, Antarctic Climate & Ecosystems Cooperative Research Centre, Hobart, Tasmania, 2010.

760

Gupta, G. V. M., Jyothibabu, R., Ramu, C. V., Reddy, A. Y., Balachandran, K. K., Sudheesh, V., Kumar, S., Chari, N. V. H. K., Bepari, K. F., Marathe, P. H. and Reddy, B. B.: The world's largest coastal deoxygenation zone is not anthropogenically driven, Environmental Research Letters, 16(5), p.054009, 2021.

765

Hartstein, N. D.: Supply and dispersal of mussel farm debris and its impacts on benthic habitats in contrasting hydrodynamic regimes, PhD thesis, University of Auckland, 2003.

Hartstein, N., Maxey, J. D., & Kerroux, A.: ~~(2016)~~ Potential Causes of Beggiatoa Coverage in and Around Franklin Lease and Macquarie Harbour, a Report to the Tasmanian Salmonid Growers Association from²² Aquadynamic Solutions Sdn. Bhd., Kota Kinabalu, Sabah, Malaysia, 2016.

770

Hartstein, N. D., Maxey, J. D., Loo, J. C. H., & Then, A. Y. H.: Drivers of deep water renewal in Macquarie Harbour, Tasmania, Journal of Marine Systems, 199, 103226, 2019.

775

Hemer, M. A., & Griffin, D. A. ~~(2010)a~~: The wave energy resource along Australia's Southern margin. Journal of Renewable and Sustainable Energy, 2(4), 043108, 2010a.

Hemer, M. A., Church, J. A., & Hunter, J. R. ~~(2010)b~~: Variability and trends in the directional wave climate of the Southern Hemisphere. International Journal of Climatology: A Journal of the Royal Meteorological Society, 30(4), 475-491, 2010b.

780

Hill, K. J., Santoso, A., & England, M. H. ~~(2009)~~: Interannual Tasmanian rainfall variability associated with large-scale climate modes. Journal of Climate, 22(16), 4383-4397, 2009.

785

Inall, M. E., & Gillibrand, P. A.: ~~(2010)~~ The physics of mid-latitude fjords: a review. Geological Society, London, Special Publications, 344(1), 17-33, 2010.

Ji, Q., Frey, C., Sun, X., Jackson, M., Lee, Y. S., Jayakumar, A., Cornwell, J. C. and Ward, B. B.: ~~(2018)~~ Nitrogen and oxygen availabilities control water column nitrous oxide production during seasonal anoxia in the Chesapeake Bay. Biogeosciences, 15(20), pp.6127-6138, 2018.

790

Ji, Q., Jameson, B. D., Juniper, S. K., & Grundle, D. S.: ~~(2020)~~. Temporal and vertical oxygen gradients modulate nitrous oxide production in a seasonally anoxic fjord: Saanich Inlet, British Columbia. *Journal of Geophysical Research: Biogeosciences*, 125(9), e2020JG005631, [2020](https://doi.org/10.1029/2020JG005631).

795

[Keeling, R. F., Körtzinger, A., & Gruber, N.: Ocean deoxygenation in a warming world. *Annual Review of Marine Science*, 2, 199-229, 2010.](https://doi.org/10.1146/annurev-marine-010810-094911)

800

Keith, D. A., Ferrer-Paris, J. R., Nicholson, E. and Kingsford, R. T. (eds.) ~~(2020)~~. The IUCN Global Ecosystem Typology 2.0: Descriptive profiles for biomes and ecosystem functional groups. Gland, Switzerland: IUCN. <https://doi.org/10.2305/IUCN.CH.2020.13.en>, 2020.

805

Kiernan, K. ~~(1990)~~. The Extent of Late Cenozoic Glaciation in the Central Highlands of Tasmania, Australia. *Arctic and Alpine Research*, 22(4), 341–354. <https://doi.org/10.2307/1551459>, 1990.

810

Kiernan, K.: ~~(1991)~~ Glacial history of the upper Derwent Valley, Tasmania, *New Zealand Journal of Geology and Geophysics*, 34:2, 157-166, DOI:10.1080/00288306.1991.9514453, 1991.

Kiernan, K. ~~(1995)~~. A reconnaissance of the geomorphology and glacial history of the upper Gordon River Valley, Tasmania. *Tasforests*, 7, 51-76. [1995](https://doi.org/10.1080/14498599508839111).

815

King, R. D.: ~~(1980)~~. Limnology of the Gordon River Basin, Tasmania, and its meromictic lakes. (Doctoral Dissertation, University of Tasmania). 1980.

King, R. D., & Tyler, P. A.: ~~(1981)~~. Meromictic lakes of south-west Tasmania. *Marine and Freshwater Research*, 32(5), 741-756, [1981](https://doi.org/10.1080/00288306.1981.10555555).

820

King, R. D., & Tyler, P. A. ~~(1982)~~. Downstream effects of the ~~Gorden~~Gordon River Power Development, south-west Tasmania. *Marine and Freshwater Research*, 33(3), 431-442, [1982](https://doi.org/10.1080/00288306.1982.10555555).

Kirkpatrick, J. B., Nunez, M., Bridle, K. L., Parry, J., Gibson, N.: ~~(2017)~~. Causes and consequences of variation in snow incidence on the high mountains of Tasmania, 1983–2013. ~~Aust~~*Australian Journal of Botany*, 65, 214–224. <https://doi.org/10.1071/BT16179>, 214–224, 2017.

Formatted: Default Paragraph Font

Formatted: Default Paragraph Font

Formatted: Default Paragraph Font

825 Koehnken, L.: ~~(1996)~~ Water Quality in the King River and Macquarie Harbour, Tasmania: Pre-and Post-Mount Lyell Mine Closure. In Hydrology and Water Resources Symposium 1996: Water and the Environment; Preprints of Papers (p. 157). Institution of Engineers, Australia. ~~1996~~.

830 Lam, P., & Kuypers, M. M.: ~~(2011)~~ Microbial nitrogen cycling processes in oxygen minimum zones. Annual review of marine science, 3, 317-345. ~~(2011)~~.

[Levin, L. A., & Breitburg, D. L.: Linking coasts and seas to address ocean deoxygenation, Nature Climate Change, 5\(5\), 401-403, 2015.](#)

835 Liu, L., Wilkinson, J., Koca, K., Buchmann, C., & Lorke, A.: ~~(2016)~~ The role of sediment structure in gas bubble storage and release. Journal of Geophysical Research: Biogeosciences, 121(7), 1992-2005. ~~2016~~.

Lucieer, V.: ~~anessa, Dr (2007)~~ SeaMap Tasmania Bathymetric Data [\[data set\]](#). Institute for Marine and Antarctic Studies, University of Tasmania. ~~2007-(dataset)~~.

840

Macquarie Harbour Dissolved Oxygen Working Group (October 2014). Final Report to the Tasmanian Salmonid Growers Association ~~(TSGA), 2014~~

845 Marshall, ~~Gareth G.~~ & National Center for Atmospheric Research Staff (Eds): ~~Last modified 19 Mar 2018.~~ "The Climate Data Guide: Marshall Southern Annular Mode (SAM) Index (Station-based)." Retrieved from <https://climatedataguide.ucar.edu/climate-data/marshall-southern-annular-mode-sam-index-station-based>, ~~Last modified 19 Mar 2018,~~ (Accessed 20th January 2022.)

850 Mau, S., Bles, J., Helmke, E., Niemann, H., & Damm, E.: ~~(2013)~~ Vertical distribution of methane oxidation and methanotrophic response to elevated methane concentrations in stratified waters of the Arctic fjord Storfjorden (Svalbard, Norway). Biogeosciences, 10(10), 6267-6278. ~~2013~~.

855 Maxey, J. D., Hartstein, N. D., Penjinus, D., & Kerroux, A.: ~~(2017)~~ Simple quality control technique to identify dissolved oxygen diffusion issues with biochemical oxygen demand bottle incubations. Borneo Journal of Marine Science and Aquaculture (BJoMSA), ~~1, 2017~~.

Formatted: Default Paragraph Font

Maxey, J. D., Hartstein, N. D., Then, A. Y. H., & Barrenger, M. ~~(2020)~~. Dissolved oxygen consumption in a fjord-like estuary, Macquarie Harbour, Tasmania. *Estuarine, Coastal and Shelf Science*, 246, 107016. [2020](#).

860 Meneghini, B., Simmonds, I., & Smith, I. N. ~~(2007)~~. Association between Australian rainfall and the southern annular mode. *International Journal of Climatology: A Journal of the Royal Meteorological Society*, 27(1), 109-121. [2007](#).

Oschlies, A., Brandt, P., Stramma, L., & Schmidtko, S. ~~(2018)~~. Drivers and mechanisms of ocean deoxygenation. *Nature Geoscience*, 11(7), 467-473. [2018](#).

865

Pereira, P. M., Black, K. D., McLusky, D. S., & Nickell, T. D. ~~(2004)~~. Recovery of sediments after cessation of marine fish farm production. *Aquaculture*, 235(1-4), 315-330. [2004](#).

Pickard, G. L., & Stanton, B. R. ~~(1980)~~. Pacific fjords-a review of their water characteristics. *Fjord Oceanography*, 1-51. [1980](#).

870

Pitcher, G. C., Aguirre-Velarde, A., Breitburg, D., Cardich, J., Carstensen, J., Conley, D. J., Dewitte, B., Engel, A., Espinoza-Morriberón, D., Flores, G. and Garçon, V., Graco, M., *et al.* ~~(2021)~~. System controls of coastal and open ocean oxygen depletion. *Progress in Oceanography*, p.102613. [2021](#).

875

Priestley, M. D., & Catto, J. L. ~~(2021)~~. Future changes in the extratropical storm tracks and cyclone intensity, wind speed, and structure. *Weather and Climate Dynamics Discussions*, 1-40. [2021](#).

Rabalais, N. N., Diaz, R. J., Levin, L. A., Turner, R. E., Gilbert, D., & Zhang, J. ~~(2010)~~. Dynamics and distribution of natural and human-caused hypoxia. *Biogeosciences*, 7(2), 585-619. [2010](#).

880

Reeburgh, W. S. ~~(2007)~~. Oceanic methane biogeochemistry. *Chemical Reviews*, 107(2), 486-513. [2007](#).

Rosenberg, R. ~~(1977)~~. Benthic macrofaunal dynamics, production, and dispersion in an oxygen-deficient estuary of west Sweden. *Journal of Experimental Marine Biology and Ecology*, 26(2), 107-133. [1977](#).

885

Sharples, C., Walford, H., Watson, C., Ellison, J. C., Hua, Q., Bowden, N., & Bowman, D. ~~(2020)~~. Ocean Beach, Tasmania: A swell-dominated shoreline reaches climate-induced recessional tipping point?. *Marine Geology*, 419, 106081. [2020](#).

Formatted: Font: Italic

- 890 Skogen, M. D., Eknes, M., Asplin, L. C., & Sandvik, A. D. ~~(2009)~~. Modelling the environmental effects of fish farming in a Norwegian fjord. *Aquaculture*, 298(1-2), 70-75. [2009](#).
- Smith, R. W., Bianchi, T. S., Allison, M., Savage, C., & Galy, V. ~~(2015)~~. High rates of organic carbon burial in fjord sediments globally. *Nature Geoscience*, 8(6), 450-453. [2015](#).
- 895 Stanton, B. R., & Pickard, G. L. ~~(1980)~~. Physical oceanography of the New Zealand fjords. *In Fjord oceanography, edited by: Freeland, H. J., D. M. Farmer, C. D. Levings, Springer, Boston, MA, 453-489, ISBN: 978-1-4613-3107-0, 329-332, 1980. In Fjord oceanography (pp. 329-332). Springer, Boston, MA.*
- 900 Stauber, J. L., Benning, R. J., Hales, L. T., Eriksen, R., & Nowak, B. ~~(2000)~~. Copper bioavailability and amelioration of toxicity in Macquarie Harbour, Tasmania, Australia. *Marine and Freshwater Research*, 51(1), 1-10. [2000](#).
- Taschetto, A. S., & England, M. H. ~~(2009)~~. An analysis of late twentieth century trends in Australian rainfall. *International Journal of Climatology: A Journal of the Royal Meteorological Society*, 29(6), 791-807. [2009](#).
- 905 Teasdale, P. R., Apte, S. C., Ford, P. W., Batley, G. E., & Koehnken, L. ~~(2003)~~. Geochemical cycling and speciation of copper in waters and sediments of Macquarie Harbour, Western Tasmania. *Estuarine, Coastal and Shelf Science*, 57(3), 475-487. [2003](#).
- 910 Viney, N. R., Post, D. A., Yang, A., Willis, M., Robinson, K. A., Bennett, J. C., Ling, F. L. N., and Marvanek, S. ~~(2009)~~ Rainfall-runoff modelling for Tasmania. A report to the Australian Government from the CSIRO Tasmania Sustainable Yields Project, CSIRO Water for a Healthy Country Flagship, Australia. [2009](#).
- 915 Walinsky, S. E., Prah, F. G., Mix, A. C., Finney, B. P., Jaeger, J. M., & Rosen, G. P. ~~(2009)~~. Distribution and composition of organic matter in surface sediments of coastal Southeast Alaska. *Continental Shelf Research*, 29(13), 1565-1579. [2009](#).
- Walker, K. F. ~~(1985)~~. A review of the ecological effects of river regulation in Australia. *Perspectives in Southern Hemisphere Limnology*, 111-129. [1985](#).
- 920 Wang, Y., Hendy, I., & Napier, T. J.: Climate and anthropogenic controls of coastal deoxygenation on interannual to centennial timescales. *Geophysical Research Letters*, 44(22), 11-528. [2017](#).
- WEF, A. A. Standard Methods. ~~2005~~. Standard Methods, 3030. [2005](#).

925 Willis, M.-(2008). Tascatch Variation 2 – Surface Water Models (Document ID Number WR 2008/005). Department of
Primary Industries and Water. Hydro Tasmania Consulting. [https://nre.tas.gov.au/water/water-monitoring-and-
assessment/hydrological-assessment/tasmanian-catchments-modelling/surface-water-models](https://nre.tas.gov.au/water/water-monitoring-and-assessment/hydrological-assessment/tasmanian-catchments-modelling/surface-water-models), 2008

930 Ye, W., Zhang, G., Zheng, W., Zhang, H., & Wu, Y.: Methane distributions and sea-to-air fluxes in the Pearl River Estuary
and the northern South China sea, Deep Sea Research Part II: Topical Studies in Oceanography, 167, 34-45, 2019. Ye, W.,
Zhang, G., Zheng, W., Zhang, H., & Wu, Y. (2019). Methane distributions and sea to air fluxes in the Pearl River Estuary
and the northern South China sea. Deep Sea Research Part II:

Formatted: Default Paragraph Font